

Catheter-Based Intramyocardial Injection of Autologous Skeletal Myoblasts as a Primary Treatment of Ischemic Heart Failure

Clinical Experience With Six-Month Follow-Up

Pieter C. Smits, MD, PhD,* Robert-Jan M. van Geuns, MD, PhD,† Don Poldermans, MD, PhD,* Manolis Bountiokos, MD,* Emile E. M. Onderwater,* Chi Hang Lee, MD,* Alex P. W. M. Maat, MD,* Patrick W. Serruys, MD, PhD*

Rotterdam, The Netherlands

OBJECTIVES	We report on the procedural and six-month results of the first percutaneous and stand-alone study on myocardial repair with autologous skeletal myoblasts.
BACKGROUND	Preclinical studies have shown that skeletal myoblast transplantation to injured myocardium can partially restore left ventricular (LV) function.
METHODS	In a pilot safety and feasibility study of five patients with symptomatic heart failure (HF) after an anterior wall infarction, autologous skeletal myoblasts were obtained from the quadriceps muscle and cultured in vitro for cell expansion. After a culturing process, 296 ± 199 million cells were harvested (positive desmin staining $55 \pm 30\%$). With a NOGA-guided catheter system (Biosense-Webster, Waterloo, Belgium), 196 ± 105 million cells were transendocardially injected into the infarcted area. Electrocardiographic and LV function assessment was done by Holter monitoring, LV angiography, nuclear radiography, dobutamine stress echocardiography, and magnetic resonance imaging (MRI).
RESULTS	All cell transplantation procedures were uneventful, and no serious adverse events occurred during follow-up. One patient received an implantable cardioverter-defibrillator after transplantation because of asymptomatic runs of nonsustained ventricular tachycardia. Compared with baseline, the LV ejection fraction increased from $36 \pm 11\%$ to $41 \pm 9\%$ (3 months, $p = 0.009$) and $45 \pm 8\%$ (6 months, $p = 0.23$). Regional wall analysis by MRI showed significantly increased wall thickening at the target areas and less wall thickening in remote areas (wall thickening at target areas vs. 3 months follow-up: 0.9 ± 2.3 mm vs. 1.8 ± 2.4 mm, $p = 0.008$).
CONCLUSIONS	This pilot study is the first to demonstrate the potential and feasibility of percutaneous skeletal myoblast delivery as a stand-alone procedure for myocardial repair in patients with post-infarction HF. More data are needed to confirm its safety. (J Am Coll Cardiol 2003; 42:2063-9) © 2003 by the American College of Cardiology Foundation

Cell transplantation is emerging as a potential novel therapeutic approach for the treatment of heart failure (HF). Initial studies with different cell types have shown promising results of cell transplantation in ischemic animal models.

See page 2070

Most preclinical experience has been reported on transplantation of skeletal myoblasts in infarcted myocardium. These studies demonstrated that transplanted skeletal myoblasts in damaged myocardium are capable of cellular engraftment, myotube formation, expression of the slow fiber marker beta-myosin heavy chain, long-term graft survival, and augmentation of ventricular function (1-6). As a result of the outcomes of these animal studies, a pilot safety and

feasibility study on percutaneous transplantation of autologous skeletal myoblasts by transendocardial injection as a stand-alone procedure in five patients with ischemic HF was completed. We report on the procedural and six-month follow-up results.

PROCEDURE

Objectives. The primary objectives of this pilot study are feasibility and safety at six months. The secondary objective was to assess improvement of the left ventricular (LV) function by iterative investigations at baseline and one, three, and six months. The protocol was approved by the local medical ethics committee, and written, informed consent was obtained from all patients.

Patient selection. Only symptomatic patients with New York Heart Association functional class \geq II under optimal medical therapy were selected. All patients were known to have a previous anterior wall myocardial infarction and depressed LV function (left ventricular ejection fraction

From the *Department of Cardiology, Thorax Center; and the †Department of Radiology, Erasmus Medical Center, Rotterdam, The Netherlands. This study was partly financially supported by Bioheart Inc., Weston, Florida.

Manuscript received April 16, 2003; accepted June 4, 2003.

Abbreviations and Acronyms

DSE	=	dobutamine stress echocardiography
ECG	=	electrocardiogram
HF	=	heart failure
ICD	=	implantable cardioverter-defibrillator
LAO	=	left anterior oblique
LV	=	left ventricle/ventricular
LVEF	=	left ventricular ejection fraction
MRI	=	magnetic resonance imaging
NSVT	=	non-sustained ventricular tachycardia
RAO	=	right anterior oblique
TDI	=	tissue Doppler imaging

[LVEF] between 20% and 45% by radionuclide radiography). Myocardial infarction had to be >4 weeks old at the time of implantation. The presence and location of a myocardial scar were defined by: akinesia or dyskinesia at rest during echocardiography, LV angiography, and magnetic resonance imaging (MRI); no contractile reserve during dobutamine stress echocardiography (DSE); and hyperenhancement by gadolinium on the MRI scan. Exclusion criteria for myoblast injections were: target region wall thickness <5 mm by echocardiography or MRI; a history of syncope or sustained ventricular tachycardia or fibrillation or (potential candidate for) implantable cardioverter-defibrillator (ICD) placement; and positive serologic test results for human immunodeficiency virus, hepatitis B or C, or syphilis.

Muscle biopsy. Biopsy of the quadriceps muscle was done under local anesthesia. On average, 8.4 g (range 5 to 13 g) of muscle biopsy was excised through a 10-cm-long surgical incision. All five biopsy procedures were uneventful and done on an outpatient basis. Biopsies were placed in a bottle containing a proprietary solution designed to preserve the biopsy during controlled shipment. The bottle was put in an insulated thermobox with frozen and refrigerated gel packs to maintain temperatures between 2°C and 8°C during transit. The transport conditions were monitored by the use of a programmable temperature monitor (Sensitech, Beverly, Massachusetts). The container was sent to clinical Good Manufacture Practice (BioWhittaker, Cambrex Corp., Walkersville, Maryland) for myoblast cell isolation and expansion. The average transit duration was 41 h (range 35 to 50 h); no temperature excursions were noted.

Cell-culturing process. On receipt at the culturing facility, the biopsies were processed according to the Myocell protocols by Bioheart Inc. The biopsy was minced finely and then dissociated using digestive enzymes. The dissociated tissue was washed several times and filtered until a single-cell suspension was achieved. The expansion culture was initiated when the cells were plated into sterile tissue culture flasks in growth media for skeletal muscle myoblasts. The media were changed at regular intervals; the cells were harvested and replated according to cell confluence parameters. Final harvest was done after three to five passages. Myoblasts were identified using an immunohistochemical

marker specific for desmin (DAKO) to identify cells committed to a myogenic differentiation. Specific cell lot release specifications (cell viability, cell identity, and sterility tests) were established before the start of the trial, which, if not met, would result in a re-biopsy of the patient and re-initiation of the culture process. In three patients a re-biopsy was required due to the desmin staining results falling below the lot release criteria. In these patients, a prestimulation procedure was performed using multiple needle punctures of the muscle three days before the biopsy procedure to increase the percentage of myoblast cells in the muscle biopsy (7).

After a culturing period of 17 days (range 14 to 19 days), the harvested cells were formulated in a specially designed transport/injectate media and transferred into a sterile 30-ml bag and sent to our hospital. Shipment was done under the same controlled conditions as after biopsy. The transit time averaged 62 h (range 24 to 96 h), and no temperature excursions were noted. The cells have been validated for having a 96-h shelf life under controlled conditions.

Transplantation procedure. The transplantation procedure was scheduled the day after arrival of the cells. Cell transplantation was done in the cardiac catheterization laboratory. Access was obtained through the femoral artery, and 100 IU/kg heparin was given. The target activated clotting time was between 250 s and 300 s and was regularly checked every half hour. After a coronary and biplane LV angiogram (left anterior oblique [LAO] 60° and right anterior oblique [RAO] 30°) was obtained, an outline of the LV chamber was drawn on transparent tabloids that were taped to the fluoroscopy monitors. Then an electromechanical NOGA map (8) of the LV was obtained using a 7F NOGASTAR catheter (F-curve) connected to the NOGA console (Biosense-Webster, Waterloo, Belgium). Areas exhibiting low voltages and linear local shortening (unipolar voltage <4 mV and linear local shortening <4%) on the NOGA map were considered as the target areas of treatment if these areas were geographically concordant with the scar areas assessed by the preprocedural DSE, MRI, and LV angiogram. We refrained from transendocardial injections into areas with a known wall thickness <5 mm by MRI. With an 8F MYOSTAR (Biosense-Webster) injection catheter, 16 ± 4 (mean ± SD; range 9 to 19) transendocardial injections were made. The catheter has nitinol tubing that ends in a 27-gauge retractable needle. Depending on the average wall thickness of the target region, the needle length was set at 4.5 to 6.0 mm when the catheter tip had a 90° curve. By connecting a 1-ml Luer-Lok syringe to the injection port, the catheter was preloaded with the skeletal myoblast solution. After establishing stable endomyocardial contact on the NOGA map and fluoroscopy, the needle was advanced manually, which often caused ventricular extra beats. Whenever a regular electrocardiographic (ECG) rhythm resumed with persisting, stable endomyocardial contact, injections of 0.3 ml (16.6 million cells) were

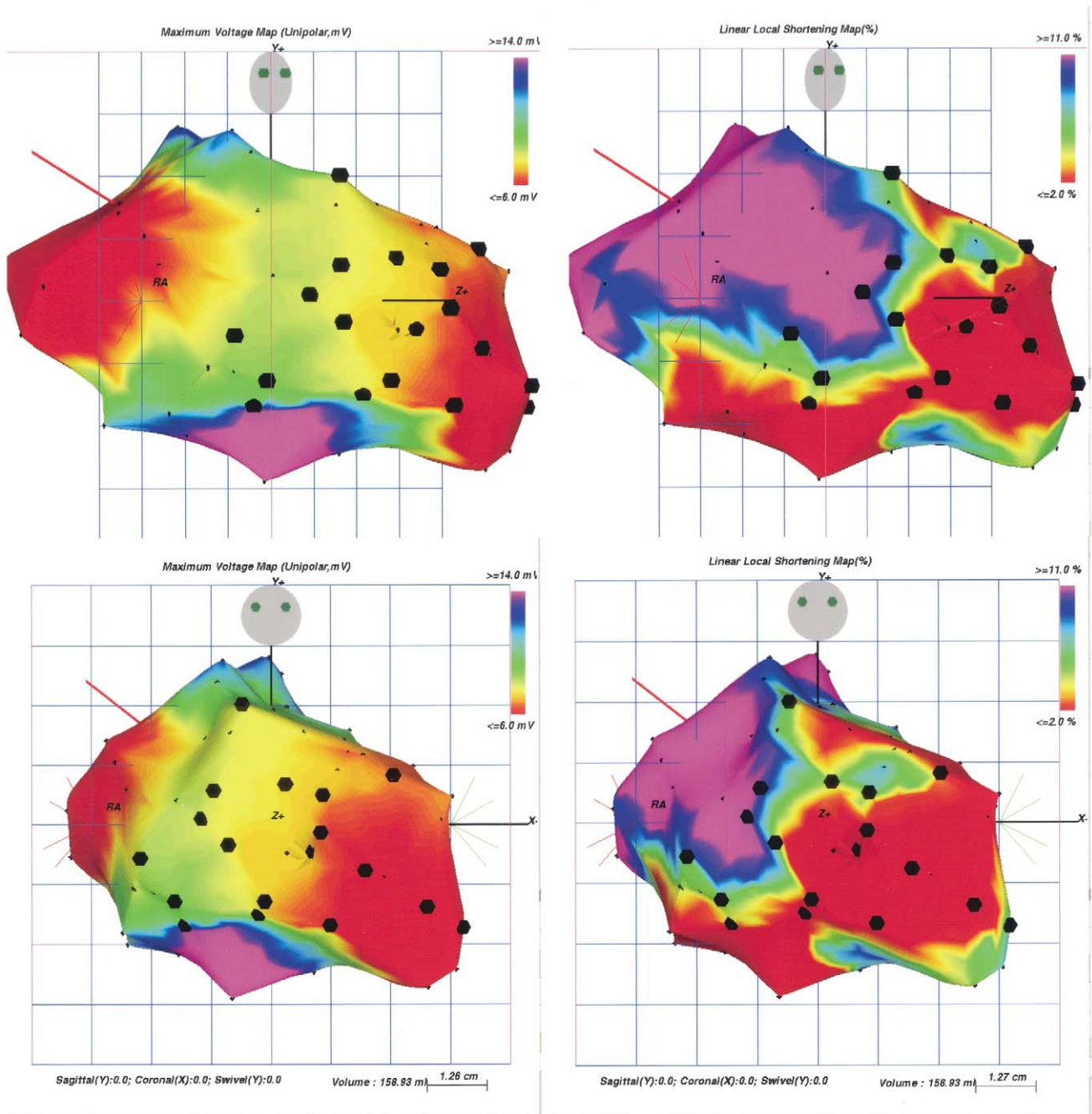


Figure 1. NOGA maps (left = unipolar voltage maps; right = linear local shortening maps) in the right anterior oblique (top) and anteroposterior (bottom) views of Patient no. 2 after 19 injections with autologous skeletal myoblasts in the anteroseptal and anterior myocardial scar and border zone. The myocardial scar is indicated in red on the unipolar voltage map (<6 mV) and on the local linear shortening map (<2%). The black dots indicate the transcatheter injection sites.

made. Only the first patient received 0.1-ml injections (2.5 million cells) because of the limited volume of myoblast solution. Injection sites were marked on the NOGA map (Fig. 1) and the transparent tabloids. Spacing between injection sites was approximately 1.0 cm apart. After the injection procedure, a control biplane LV angiogram was obtained. Afterward, patients were ECG monitored for 18 h, and cardiac enzymes were checked twice at 6- to 8-h

intervals. In all five cases, the in-hospital stay was uneventful, and the patients were discharged within 24 h after the procedure.

Methods of assessment. At baseline and one, three, and six months of follow-up, 24-h ambulant ECG monitoring and DSE with pulsed-wave tissue Doppler imaging (TDI) were done. The DSE and TDI procedures were performed with a Hewlett-Packard Sonos 5500 (Andover, Massachu-

Table 1. Patient and Cell Culture Characteristics

Pt. No.	Gender, Age (yrs)	Previous Anterior AMI (years ago)	NYHA Class	Patent LAD	Known Arrhythmias	Cells at Harvest × 10 ⁶	Cells Injected × 10 ⁶	Desmin Staining (%)	Cell Viability (%)	Potency (%)
1	F, 78	6	III	Yes	PAT runs	25	25	85	98	90
2	M, 53	3	II/III	Yes	PAT runs	544	293	12	97	20-40
3	M, 55	11	III/IV	No*	PAF, NSVT runs†	183	183	54	95	70
4	M, 59	7	III	Yes	No	211	211	80	95	100
5	M, 49	2	III	Yes	No	382	270	44	98	40

*LAD filled by collateral channels. †Asymptomatic, 8 complexes.

AMI = acute myocardial infarction; LAD = left anterior descending coronary artery; NSVT = non-sustained ventricular tachycardia runs; NYHA = New York Heart Association; PAF = paroxymal atrial fibrillation; PAT = paroxymal atrial tachycardia.

setts) imaging system equipped with second harmonic imaging to optimize endocardial border detection and performed as previously described (9,10). In short, after baseline echocardiography, dobutamine was infused at a starting dose of 5 µg/kg/min for 5 min, followed by 10 µg/kg/min for 5 min (low-dose stage). Dobutamine was then increased by 10 µg/kg/min every 3 min up to a maximum dose of 40 µg/kg/min. Atropine (1 to 2 mg) was added at the end of the last stage if the target heart rate had not been achieved. Images were acquired continuously and recorded on tape at the end of every dose step. In addition, the baseline, low-dose, peak stress, and recovery images (standard apical and short-axis views) were displayed in a cine loop format. Wall motion was scored according to the criteria of the American Society of Echocardiography by two experienced reviewers blinded to the MRI data for systolic wall thickening. Pulsed-wave TDI was performed with a Hewlett-Packard Sonos 5500, and a transducer operating at frequencies of 1.8 or 2.1 MHz with a pulse repetition frequency of 45 to 60 kHz was used. Using a six-segment model, pulsed-wave TDI was performed close to the mitral annulus in the apical four-chamber, apical two-chamber, and apical three-chamber views with high temporal resolution (4 ± 3 ms; range 1 to 7). The depth of the sample volume was kept constant in each patient during DSE. A sample volume with a fixed length of 4 mm was used. The ECG and phonocardiogram were simultaneously recorded with the pulsed-wave TDI velocity profile and stored on videotape. The peak pulsed-wave TDI velocity amplitude of the ejection phase and early and late diastole were measured off-line using a computer-assisted drawing system, and the values were expressed in cm/s (10). Five consecutive beats were analyzed, and the mean velocity values were calculated to minimize the measurement variability determined by respiration. The E/A ratio was also calculated. Cardiac cycles with extrasystolic or postextrasystolic beats or any disturbance of the rhythm were excluded. Recordings and measurements were repeated at baseline and at a low-dose (10 µg/kg/min) dobutamine infusion rate.

Furthermore, at baseline and three and six months of follow-up, the LV volume and LVEF were assessed by biplane LV angiography and technetium-99m-labeled erythrocyte radionuclide scintigraphy. Biplane LV angiography was done in the LAO 60° and RAO 30° projections

with 100-ml sphere calibration in the isocenter. Quantitative analysis was performed using CAAS II software (Pie Medical, Maastricht, The Netherlands). Also, at baseline and three-month follow-up, a MRI scan of the heart was obtained. The studies were performed on a 1.5-T whole-body MRI system (Sonata, Siemens, Erlangen, Germany). Patients were placed in a supine position with a four-channel quadrature body phased-array coil placed over the thorax. For quantitative analysis, multiple parallel short-axis slices covering the heart from base to apex were obtained using a ECG-triggered breath-hold cine gradient-echo sequence. Imaging parameters were: repetition time of 3.2 ms, echo time of 1.6 ms, and flip angle 65°, which resulted in a temporal resolution of 47 ms. Quantitative analysis was performed using standardized software (Argus Siemens, Erlangen, Germany). Endocardial and epicardial contours were traced using semi-automatic software to calculate the LV volumes and LVEF. Each short-axis image was divided into eight segments of 45°, which resulted in 64 to 80 segments per patient, depending on the number of short-axis slices covering the heart from base to apex. Regional wall thickening was calculated for each segment by subtracting the end-diastolic wall thickness from the end-systolic wall thickness. Delayed contrast-elucidated MRI images were used to identify transmural and nontransmural infarcts using a three-dimensional inversion-recovered gradient echo sequence 15 min after injection of 0.1 mmol gadolinium-based contrast agent.

RESULTS

Baseline patient characteristics and cell-culturing results are summarized in Table 1. No procedural complications occurred. Only in one patient (Patient no. 5) was minor elevation of creatine kinase and its MB fraction (<2 times upper level) and troponin T (0.16 µg/l) noted after the procedure.

During follow-up, Patient no. 3 needed to be hospitalized at six weeks after the procedure due to progressive HF and long asymptomatic runs of non-sustained ventricular tachycardia (NSVT) on Holter monitoring. After recompensation, telemetry still showed NSVT, and an ICD was implanted prophylactically. In the other four patients, no adverse events or ventricular arrhythmias were observed.

Table 2. Global Left Ventricular Function Results

Pt. No.	Baseline			3-Month Follow-Up			6-Month Follow-Up		
	LVEF (%) by Angiography (EDV/ESV)	LVEF (%) by Nuclear Radiography	LVEF (%) by MRI (EDV/ESV)	LVEF (%) by Angiography (EDV/ESV)	LVEF (%) by Nuclear Radiography	LVEF (%) by MRI (EDV/ESV)	LVEF (%) by Angiography (EDV/ESV)	LVEF (%) by Nuclear Radiography	LVEF (%) by MRI (EDV/ESV)
1	43 (187/107)	39	36 (189/120)	47 (203/108)	42	41 (190/113)	54 (200/93)	56	54 (200/93)
2	40 (135/82)	45	43 (167/96)	42 (150/87)	40	37 (166/104)	49 (156/80)	39	49 (156/80)
3	18 (153/126)	32	22 (169/132)	26 (148/109)	26	25 (166/125)	46 (150/82)	42	46 (150/82)
4	40 (201/120)	36	26 (206/152)	44 (195/110)	31	24 (202/154)	33 (211/141)	32	33 (211/141)
5	42 (141/83)	37	35 (125/82)	47 (119/64)	40	37 (132/82)	43 (129/43)	57	43 (129/43)
Average	36 ± 11 (163 ± 29/103 ± 21)	38 ± 5	32 ± 8 (171 ± 30/116 ± 28)	41 ± 9* (163 ± 35/95 ± 20)	36 ± 7	33 ± 8 (171 ± 27/116 ± 26)	45 ± 8 (169 ± 35/94 ± 27)	45 ± 11	45 ± 11

*p = 0.009.

EDV and ESV = end-diastolic and end-systolic volume, respectively; LVEF = left ventricular ejection fraction; MRI = magnetic resonance imaging.

Global LV function results at three- and six-month follow-up are summarized in Table 2. Compared with baseline, angiographic LVEF at three months increased from 36 ± 11% to 41 ± 9% (p = 0.009). This increase in LVEF, however, was not observed by nuclear or MRI assessment at three-month follow-up. At six-month follow-up, both angiographic and nuclear LVEF assessments showed a trend toward increased LVEF (36 ± 11% to 45 ± 8% [p = 0.23] and 38 ± 8% to 45 ± 11% [p = 0.07], respectively).

The MRI analysis of regional wall thickening showed a descriptive shift toward more regional wall thickening in the target segments and less regional wall thickening in the remote hyperkinetic segments (Figs. 2 and 3). By comparing the marked injection sites on the NOGA map and the fluoroscopy sheets with the MRI segments, 87 of the 304 MRI segments (all 5 patients) were identified as injected segments. Paired analysis of these injected segments showed significantly increased wall thickening at follow-up (0.9 ± 2.3 mm at baseline vs. 1.8 ± 2.4 mm at 3-month follow-up, p = 0.008).

In all five patients at baseline, DSE showed no signs of ischemia or ventricular tachycardias. Compared with baseline, the TDI results of the target antero-septal and anterior wall showed a trend toward increased contraction velocity at six-month follow-up (antero-septal wall: 5.4 ± 1.9 cm/s vs. 6.1 ± 0.8 cm/s at rest and 8.8 ± 3.4 cm/s vs. 9.1 ± 2.5 cm/s at low-dose dobutamine; anterior wall: 5.2 ± 1.9 cm/s vs. 5.9 ± 0.7 cm/s at rest and 6.7 ± 1.7 vs. 7.5 ± 1.6 cm/s at low-dose dobutamine).

DISCUSSION

Treatment of ischemic HF remains a problem. A significant proportion of patients with congestive HF remain symptomatic despite maximal medication. Alternative therapies, including surgical cardiomyoplasty, resynchronization therapy, LV assist device, and cardiac transplantation, have their own indications and limitations. Cell transplantation has emerged as a potential new treatment strategy. Different cell types have been used for transplantation in initial preclinical experiments, but to date, most experience has been accumulated with skeletal myoblasts. There are several features that make skeletal myoblasts an attractive cell type for cardiac cell transplantation. Skeletal myoblasts can easily be obtained in sufficient quantity directly from the patient (autologous), negating the problems of organ shortage, ethical concerns, and immunosuppressive therapy. Skeletal myoblasts are relatively more resistant to ischemia than cardiomyocytes, thus favoring cellular engraftment within the ischemic or infarcted myocardium. Furthermore, the capillary density of infarcted myocardium resembles the environment in which normal skeletal muscle is obtained. The biopsy procedure is mildly invasive, and patients can be discharged within 1 h after the procedure. Although skeletal myoblasts are not cardiomyocytes, in vitro studies and in vivo observations have shown that these cells can transform

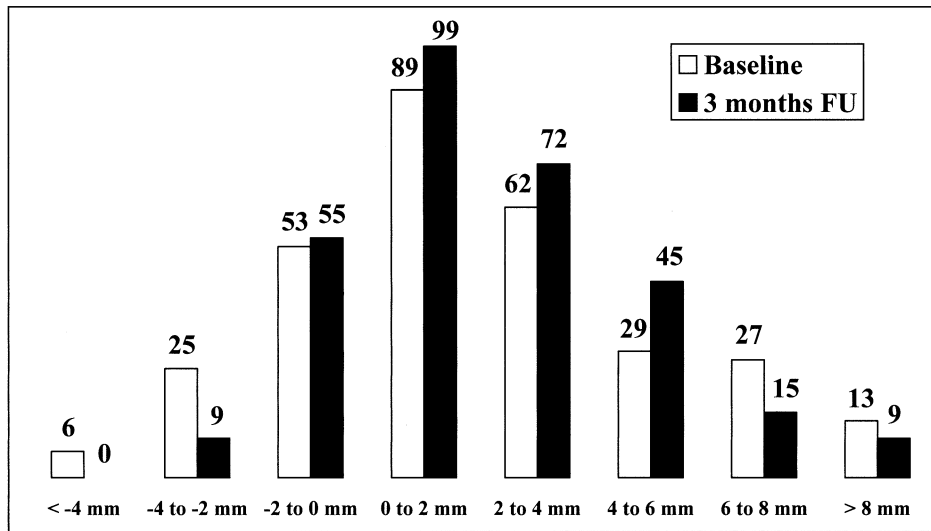


Figure 2. Changes in regional wall thickening for all 304 magnetic resonance imaging segments. The **open and solid bars** indicate the number of segments with wall thickening at baseline and three-month follow-up (FU), respectively. Compared with baseline, less segments showed thinning and more segments showed moderate thickening at three-month follow-up, and less segments with greater wall thickening were observed at that point.

into contractile cells with expression of beta-myosin heavy chain, like cardiomyocytes (6,11). The major limitation, however, is the lack of evidence of electromechanical coupling between the grafted myoblasts and the native cardiomyocytes *in vivo* (11), as well as the potential danger of inducing a reentry circuit for ventricular arrhythmias by the formed grafted myotubes in the scarred myocardium. It is known that skeletal myoblasts lose their capability to express major adhesion and gap junction proteins like N-cadherin and connexin-43, which are essential for electromechanical coupling, when the cells differentiate into myotubes (11).

We report on the first five percutaneous and stand-alone cellular cardiomyoplasty procedures as a potential new

treatment modality for ischemic HF. In post-myocardial infarction patients with LVEF <45% and symptoms of HF, autologous skeletal myoblasts were injected into the scarred myocardium by an injection catheter. No periprocedural complications occurred, and during a 3- to 12-month follow-up period, in one case, an ICD was implanted at 2 months based on a prophylactic indication because of asymptomatic NSVT runs. At three-month follow-up, in all five patients, a significant moderate increase in global LV function by LV angiography was noted. This angiographic LVEF improvement, however, was not consistently observed in all patients by nuclear or MRI assessment. Because MRI and, to a lesser extent, radionuclide angiography have

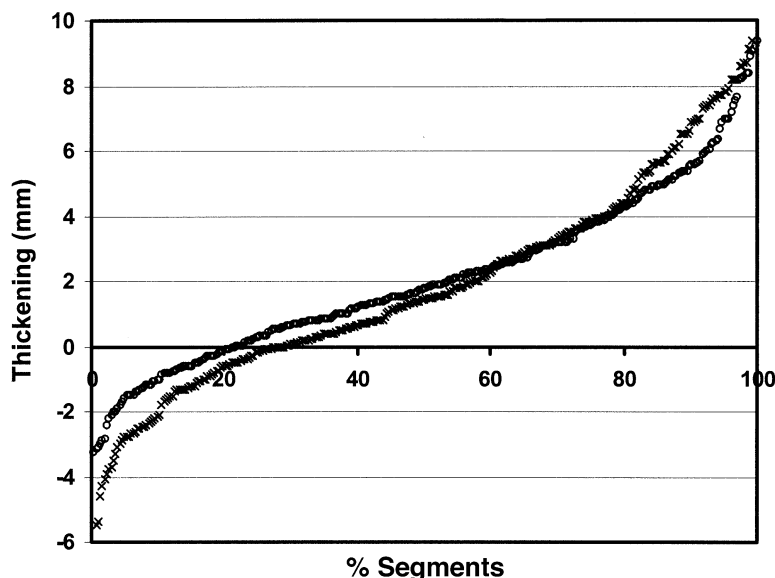


Figure 3. Cumulative distribution of regional wall thickening segments by magnetic resonance imaging at baseline (**open circles**) and three-month follow-up (**x**). At follow-up, there was a descriptive shift toward less thinning and moderate thickening in the target regions and less thickening in the normokinetic and hyperkinetic remote areas, indicating a kind of left ventricular remodeling.

been recently recognized as the most reliable and accurate methods for assessment of LV dimensions and function (12,13), cellular cardiomyoplasty efficacy studies focusing on change in LVEF should incorporate one or both of these techniques.

Regional analysis by MRI showed a significant increase in wall thickening at the target areas at three-month follow-up in all five patients. This paradox between equal global and improved regional LV function is probably explained by the remodeling of the LV, in which regional improvement of injected dyskinetic and akinetic segments is counterbalanced by less thickening of the hypercontractile remote segments, as seen by MRI. Potentially, less neurohormonal stimulation after treatment may also have occurred, resulting in less vigorous contraction of normal segments and less dyskinesia of infarcted segments. One of the limitations in our functional assessment is the missing information on the pulse-pressure double product at the different assessment time points. Pressure-volume loop and neurohormonal marker measurements in future may overcome this limitation.

Feasibility and safety. We cannot draw firm conclusions from this initial experience, but we believe that catheter-based cell transplantation in HF patients is feasible and that the transendocardial catheter-based cell delivery technique is safe from a procedural point of view. An important question about potential arrhythmogenic properties of skeletal myoblast transplantation is still unanswered. Although no syncope or malignant arrhythmias were observed in our pilot study, we have observed in two consecutive follow-up studies on catheter-based autologous skeletal myoblast transplantation in eight patients, two sudden deaths and three ventricular arrhythmias (one symptomatic and two asymptomatic) within three months after the procedure (unpublished data, P. C. Smits, 2003). These serious adverse events necessitated elementary changes in the protocols of the consecutive studies. Currently, both phase 1 follow-up studies have restarted with enrollment of patients with ICDs and rigorous rhythm monitoring before and after the procedure.

Also, Menasché et al. (14) have reported four ICD implantations within one month after the procedure in a phase 1 trial involving transepical autologous skeletal myoblast injections during bypass surgery in 10 post-myocardial infarction patients with an average baseline LVEF of 23%. However, the arrhythmogenic incidents observed in this study and in other skeletal myoblast cell transplantation studies may also reflect the natural course of this high-risk population for arrhythmias. Furthermore, the likelihood of finding a non-sustained ventricular arrhythmia recording on serial Holter monitoring is 40% in patients with HF (15). Therefore, the question remains unanswered whether skeletal myoblast transplantation is arrhythmogenic and safe.

From this initial experience, we conclude that catheter-based cell transplantation with autologous skeletal myo-

blasts for the treatment of ischemic HF is feasible and promising. However, extensive pre- and post-procedural monitoring studies for arrhythmias and well-defined functional parameters are needed to evaluate the safety and efficacy of cellular cardiomyoplasty procedures in the near future.

Acknowledgments

The help and support of Warren Sherman, MD, Howard B. Haines, PhD, and John M. Harvey, MPH, in this study are greatly appreciated.

Reprint requests and correspondence: Dr. Pieter C. Smits, Department of Cardiology, Thorax Center, Room Bd 412, Erasmus Medical Center Rotterdam, Dr. Molewaterplein 40, 3015 GD Rotterdam, The Netherlands. E-mail: p.c.smits@erasmusmc.nl.

REFERENCES

1. Chiu RC-J, Zibatis A, Kao RL. Cellular cardiomyoplasty: myocardial regeneration with satellite cell implantation. *Ann Thorac Surg* 1995; 60:12-8.
2. Taylor DA, Atkins BZ, Hungspreugs P, et al. Regenerating functional myocardium: improved performance after skeletal myoblast transplantation. *Nat Med* 1998;4:929-33.
3. Pouzet B, Vilquin JT, Messas E, et al. Factors affecting functional outcome following myoblast cell transplantation. *Ann Thorac Surg* 2001;71:844-51.
4. Murry CE, Wiseman RW, Schwartz SM, et al. Skeletal myoblast transplantation for repair of myocardial necrosis. *J Clin Invest* 1996; 98:2512-23.
5. Jain M, DerSimonian H, Brenner DA, et al. Cell therapy attenuates deleterious ventricular remodeling and improves cardiac performance after myocardial infarction. *Circulation* 2001;103:1920-7.
6. Ghostine S, Carrion C, Souza LCG, et al. Long-term efficacy of myoblast transplantation on regional structure and function after myocardial repair. *Circulation* 2002;106 Suppl I:I131-6.
7. Law PK. Myoblast transfer: gene therapy for muscular dystrophy. In: *Medical Intelligence Unit*. Austin, TX: R. G. Landes Company, 1994.
8. Ben-Haim SA, Osadchy D, Schuster I, et al. Nonfluoroscopic, in vivo navigation and mapping technology. *Nat Med* 1996;2:1393-5.
9. Elhendy A, van Domburg RT, Bax JJ, et al. Optimal criteria for the diagnosis of coronary artery disease by dobutamine stress echocardiography. *Am J Cardiol* 1998;82:1339-44.
10. Rambaldi R, Poldermans D, Bax JJ, et al. Doppler tissue velocity sampling improves diagnostic accuracy during dobutamine stress echocardiography for the assessment of viable myocardium in patients with severe left ventricular dysfunction. *Eur Heart J* 2000;21:1091-8.
11. Reinecke H, MacDonald GH, Hauschka SD, et al. Electromechanical coupling between skeletal and cardiac muscle: implications for infarct repair. *J Cell Biol* 2000;149:731-40.
12. Matheijssen NA, Baur LH, Reiber JH, et al. Assessment of left ventricular volume and mass by cine magnetic resonance imaging in patients with anterior myocardial infarction intra-observer and inter-observer variability on contour detection. *Int J Card Imaging* 1996;12: 11-9.
13. Bax JJ, Lamb H, Dibbets P, et al. Comparison of gated single-photon emission computed tomography with magnetic resonance imaging for evaluation of left ventricle function in ischemic cardiomyopathy. *Am J Cardiol* 2000;86:1299-305.
14. Menasché P, Hagege AA, Vilquin JT, et al. Autologous skeletal myoblast transplantation for severe postinfarction left ventricular dysfunction. *J Am Coll Cardiol* 2003;41:1078-83.
15. Cleland JGF, Chattopadhyay S, Khand A, Houghton T, Kaye GC. Prevalence and incidence of arrhythmias and sudden death in heart failure. *Heart Fail Rev* 2002;7:229-42.